Biochemical and Biophysical Research Communications 454 (2014) 543–546

Contents lists available at ScienceDirect

Biochemical and Biophysical Research Communications

journal homepage: www.elsevier.com/locate/ybbrc

Kinesin-1 translocation: Surprising differences between bovine brain and MCF7-derived microtubules

Mitra Shojania Feizabadi [a,b,*], Yonggun Jun [b]

[a] Department of Physics, Seton Hall University, South Orange, NJ 07079, USA
[b] Developmental and Cell Biology, School of Biological Sciences, University of California, Irvine, CA 92697, USA

ARTICLE INFO

Article history:
Received 23 October 2014
Available online 30 October 2014

Keywords:
Microtubule
MCF7 cell–bovine brain cell
Kinesin-1 translocation

ABSTRACT

While there have been many single-molecule studies of kinesin-1, most have been done along microtubules purified from bovine or porcine brain, and relatively little is known about how variations in tubulin might alter motor function. Of particular interest is transport along microtubules polymerized from tubulin purified from MCF7 breast cancer cells, both because these cells are a heavily studied model system to help understand breast cancer, and also because the microtubules are already established to have interesting polymerization/stability differences from bovine tubulin, suggesting that perhaps transport along them is also different. Thus, we carried out paired experiments to allow direct comparison of *in vitro* kinesin-1 translocation along microtubules polymerized from either human breast cancer cells (MCF7) or microtubules from bovine brain. We found surprising differences: on MCF7 microtubules, kinesin-1's processivity is significantly reduced, although its velocity is only slightly altered.

1. Introduction

Microtubules are one of the intracellular components responsible for many cell functions including but not limited to cell shape, cell division, and intracellular transportations. These dynamic polymers are structured from alpha and beta tubulin heterodimers [1–5]. Anti-mitotic therapies such as taxol suppress microtubules dynamics, highlighting the importance of their dynamics in contributing to appropriate cell division. Overall, the functionality and dynamics of microtubules has been broadly studied, and the changes caused by anti-mitotic drugs have been examined through both theoretical and experimental approaches [6–10].

Intriguingly, there are multiple different tubulin isotypes, and in different types of cells these have been shown to result in microtubules with diverse distributions of beta tubulin isotypes [11–18]. This discovery then leads to further studies characterizing the role of different beta tubulin isotypes in contributing to the dynamic and mechanical parameters of microtubules, as well as to their response to anti-cancer drugs [19–28].

In addition to other cellular functions, microtubules play a central role in intra-cellular transportation. Through binding and translocation along microtubules, motor proteins such as kinesin travel along microtubules, driving transport of cargos inside cells [29–32]. There are mutual effects of motor proteins on microtubules, and vice versa. For example, Hunter et al. have showed that motor proteins influence microtubule polymerization [33]. Conversely, a recent study by Sirajuddin et al. [34] reveals that the function of some motor proteins is affected by the tubulin isotypes of the microtubule to which they attach. Collectively, the results of these studies suggest that the unique intracellular functionalities of different cells are directly tied to the special characteristics of their elements. Thus, a better understanding of translocation of motor proteins in different cells may help understand cell-specific differences in function, especially with regard to cancer, ultimately contributing to engineering more effective therapeutic agents specifically targeting motor functions in only certain environments.

Here we characterize microtubule based translocation along microtubules derived from neuronal vs. cancerous cells. Critically, the resultant microtubules thus carry significantly different distributions of beta tubulin isotypes.

2. Materials and methods

2.1. Protein preparation

2.1.1. Microtubules

Two types of microtubule used in this study includes MCF7 microtubules and bovine brain microtubules. Microtubules were

* Corresponding author at: Physics Department, Seton Hall University, 400 South Orange Ave., South Orange, NJ 07079, USA.
E-mail address: shojanmi@shu.edu (M.S. Feizabadi).

http://dx.doi.org/10.1016/j.bbrc.2014.10.119
0006-291X/

polymerized from (A) Bovine brain tubulin (Cytoskeleton, Denver, Co, Cat. TL238A). The tubulin at ~4.2 mg/ml was polymerized through incubation for 30 min in BRB80 (80 mM PIPES, pH 7.0, 0.5 mM EGTA, and 1 mM $MgCl_2$), 1.0 mM GTP, and 20 μm Taxol at 37 °C. The polymerized Bovine microtubules were then diluted in 1:100 ratio in the same buffer explained above (stabilizing buffer). (B) Human Breast Cancer Cell (MCF7) cell tubulin (Cytoskeleton, Denver, CO, Cat. H005). The tubulin at the same concentration ~4.2 mg/ml was polymerized from MCF7 tubulin. While we have not measured the polymerization parameters of MCF7 tubulin, their polymerizations are significantly different from Bovine Brain tubulin. In order to reach to microtubules with a long length, the appropriate buffer and polymerization conditions were optimized in this case. We polymerized MCF7 tubulin in BRB80 (80 mM PIPES, pH 7.0, 0.5 mM EGTA, and 1 mM $MgCl_2$), 1.5 mM GTP, 5% Glycerol, and 20 μm Taxol at 37 °C. The incubation time at this temperature was almost 120 min. However, the polymerized microtubules remained in the room temperature for another 120 min. As compared with the Bovine brain microtubules, the samples of MCF7 microtubules after polymerization were less populated. Therefore, we diluted MCF7 microtubules in the same buffer in 1:25 ratio.

2.1.2. Motor proteins

We followed the previously reported procedure: kinesin-1 solution was thawed and diluted with assay buffer (66.4 mM Pipes, pH 6.9/50 mM potassium acetate/3.4 mM $MgSO_4$/0.8 mM DTT/0.84 mM EGTA/10.1 μM Taxol). To reach to single molecule level we implemented a series of dilution where almost 33% of binding kinesin-microtubules binding can be confirmed. Also, in order to keep motors functional for several measurements during the experiment day, kinesin-1 solutions were deep frozen in liquid nitrogen after each step of dilution. The polystyrene beads (489-nm diameter; Polysciences, Warrington, PA) were incubated with the kinesin-1 in the presence of 10 μM MgATP for almost 20 min. The bead bead's stock was further diluted with 1:20 ratio in PEM. An oxygen scavenging solution (250 μg/ml glucose oxidase, 30 μg/ml catalase, 4.6 mg/ml glucose) was added to the solution of kinesin polystyrene coated beads just before they are added to the microtubules [35–37].

2.2. Sample preparation

The flow chamber was assembled by spacing a polylysine coated coverslip and a microscope slide. The Fellow chambers with narrower channels were used for the diluted MCF7 microtubules. Tissue paper was used to blot the solution out of the flow cell. Considering the width of the channel, between 15 and 25 μm of diluted microtubules were flushed and incubated to the flow chamber for 20 min. The chamber was then flushed with the stabilizing buffer containing (5 mg/ml) of Casein to compete for tubulin for possible nonspecific binding to the coverslips. The protein-bead assay was the injected to the sample. The samples were then sealed with vacuum grease and observed under microscope.

2.3. Microtubule bead visualization and data analysis

Microtubule and beads were visualized with a Nikon TE200 (Nikon 1.49 NA, 100× objective, 1.4 NA condenser, Tokyo, Japan) using differential interference contrast optics and were videotaped with a CCD camera (30 fps, Dage-MTI-100, Michigan City, IN). The beads were trapped by optical trapping technique under a low power, then placed closed to individual microtubules. Those kinesin with the proper orientations that could bind to an individual microtubule could create the movement of the trapped beads. This movements were recorded with a custom LabView program [38]. The kinesin-1 coated beads progressed in one direction on a microtubule. The bead displacements parallel to microtubules were represented the movement of kinesin-1 along individual microtubules. The data were collected and analyzed by Igro-Pro software.

The velocities are calculated based on mean ± s.d. The mean run length is calculated by fitting a decaying exponential to the histogram distribution [39].

3. Results

We characterized *in vitro* translocation of single kinesin-1 motor proteins along microtubules polymerized from human breast cancer cell tubulin, MCF7 and bovine brain. Studies were done at saturating ATP, to reflect the typical high availability of ATP *in vivo*. We used an optical trap to place single-motor beads on individual microtubules, allowing us to determine both the distribution of travel distances of single motors (processivity) and associated velocities. Two example traces of individual beads' movement along bovine brain and MCF7 microtubule are shown in Fig. 1.

When multiple traces were analyzed, we were able to make a histogram of travel distances (Fig. 2). From these histograms, via fitting exponential decays, we obtained the unloaded single-motor processivity. This was 1047 ± 0.00094 nm for bovine brain (Fig. 2A), consistent with previous reports [40]. In contrast, the unloaded processivity measured along the MCF7 microtubules was 479 ± 0.002 nm (Fig. 2B). In both cases, the bead binding ratio was less than 33%, consistent with single-motor travel. Thus, kinesin's motion along MCF7 tubulin is significantly impeded.

Because of this, we considered whether the decrease in travel was due to a difficulty in binding to the microtubules at each step.

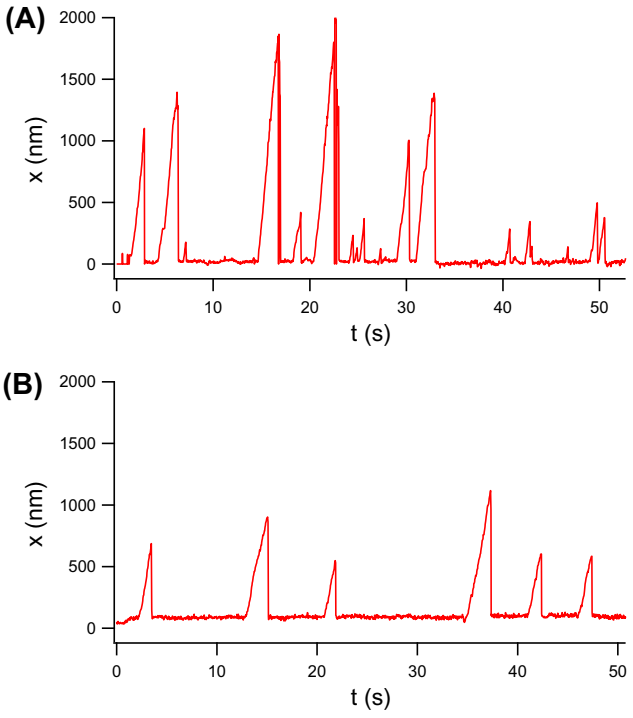

Fig. 1. Two recorded snapshots of the beads' movement along bovine brain and MCF7 microtubules are expressed as examples. The movement of the kinesin-1 coated bead along a single (A) bovine brain microtubule, (B) MCF7 microtubule is shown. The horizontal axis represents the time in the unit of second. The vertical axis represents the displacement in the unit of nm. The picks represent the detachment points of kinesin from microtubules. The experiments were conducted in the presence of 1 mM of ATP. In this case, the shorter displacement can be identified along the MCF7 microtubules, as compared to the bovine brain microtubules. This turned out to be statistically true as shown in Fig. 2.

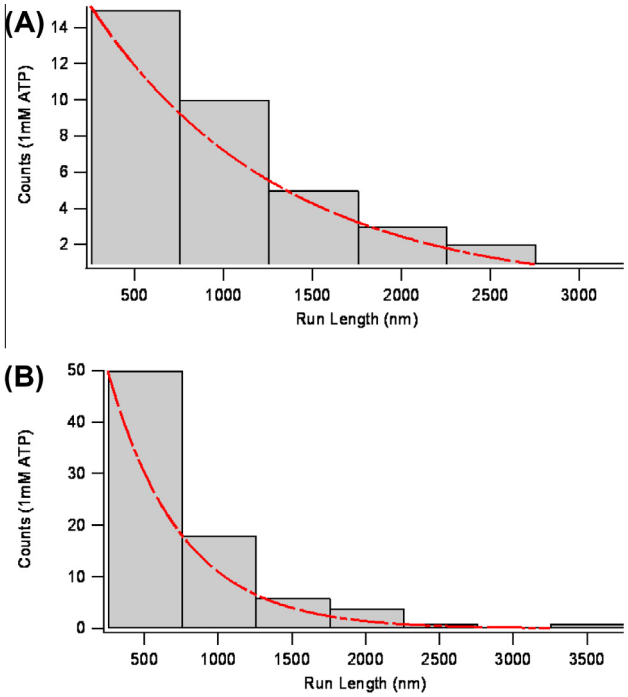

Fig. 2. The histogram of the unloaded processivity of kinesin-1 along (A) bovine brain, (B) MCF7 microtubules are shown. The histogram distribution of the measurements in both cases are fitted to a decaying exponential. The processive length is calculated from the time constant of exponential fit. The measured processivity along bovine brain microtubules is 1047 ± 0.00094 nm (n = 36 measurements, A) and for the MCF7 microtubules is 479 ± 0.002 nm (n = 80 measurements, B). In both cases, the bead binding ratio was less than 33%, consistent with single-motor travel.

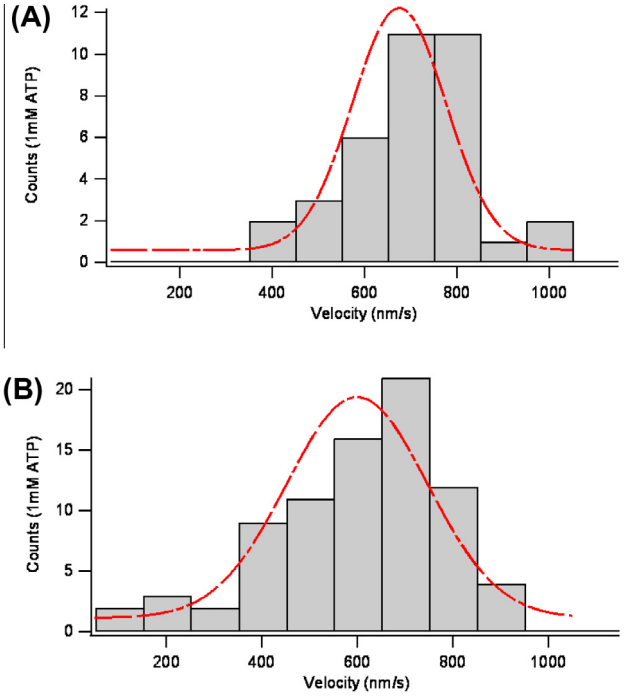

Fig. 3. The histograms express the velocity distribution of kinesin-1 along (A) bovine brain, (B) MCF7 microtubules. The average velocity of the kinesin-1is calculated by fitting the Gaussian distribution to the histograms. The obtained average velocity of kinesin-1 moving along bovine brain microtubules is 675 ± 13.3 nm/s. (n = 36 measurements, A). The similar velocity measured along MCF7 microtubules is 599 ± 16.6 (n = 80 measurements, B).

If so, we thought that this might then be reflected in a decreased velocity. To test such a model, we measured the average velocity of kinesin-1, and found it to be 675 ± 13.3 nm/s. along bovine brain microtubules (Fig. 3A), and slightly lower, 599 ± 16.6 nm/s. (Fig. 3B), along MCF7 microtubules.

4. Discussion

Recent work of Milic et al. suggests that kinesin processivity is strongly influenced by ADP release [41]. Since the motors' microtubule affinity is low when bound to ADP, a very intriguing model to account for our results is that the β-tubulin isoforms contribute to control of ADP release rate. In this model, neuronal tubulin does a better job at stimulating ADP release, resulting in a shorter portion of the enzymatic cycle occurring in the ADP-state. This decreased time in the weak binding state decreases the probability of detachment per step, improving single-motor processivity. Furthermore, by decreasing the amount of time in the ADP-portion of the cycle, the entire cycle speeds up, resulting in the small but statistically significant difference in mean velocity.

How might these different tubulin isoforms affect ADP release? Unlike neural mammalian microtubules with class II of beta tubulin as the major beta tubulin in their compositions, MCF7 microtubules are composed of 0% class II beta tubulin isotype, 39.1% class I beta tubulin isotype, 2.5% class III beta tubulin isotype and 58.4% class IV beta tubulin isotype [42]. In bovine brain microtubules beta tubulin isotypes in their structures are 3% class I, 58% class II, 25% class III, and 13% class VI [43].

The length of C-terminal and charges in the two groups of microtubules under study are different. In previously reported results of some studies, conformational differences of the C-terminal of different beta tubulin isotypes and the interaction between C-terminal and the neck domain of kinesin were suggested as critical contributors to maintain motor-microtubule contact and the distinctions that can be created in the translocation characters including average velocity and processivity [44,45]. Also in some other works, some connections between the C-terminal and the ATPase activity has also been suggested [46,47]. Therefore, while the C-terminal of tubulin may affect ADP release, the mechanism that beta tubulin isotype-specified C-terminal may change the ATPase activity, still needs to be explored.

From a biological stand point, one might wonder why the microtubules of different cells contain different tubulin isotypes. The biology of cancer cells is still poorly understood; while we know that the dimensions of these cells is much smaller than neuronal cells—so they can survive with shorter mean travels—in fact we know very little about what microtubule-based functions are particularly important for them. This finding—that transport is indeed likely to be different from normal cells—is intriguing, and we consider it an important point of departure for better understanding of the unique function of cancerous cells.

Acknowledgment

M.S.F Acknowledges the support of Seton Hall University during her sabbatical leave.

References

[1] G.G. Borisy, J.B. Olmsted, Nucleated assembly of microtubules in porcine brain extracts, Science 177 (1972) 1196–1197.
[2] G.G. Borisy, J.B. Olmsted, J.M. Marcum, C. Allen, Microtubule assembly in vitro, Fed Proc. 33 (1974) 167–174.
[3] J. Howard, Mechanics of Motor Proteins and the Cytoskeleton, Sinauer Associates, Sunderland, MA, 2001.
[4] M.W. Kirschner, T. Mitchison, Microtubule dynamics, Nature 324 (1986) 621.
[5] R.A. Walker, E.T. O'Brien, N.K. Pryer, M.F. Soboeiro, et al., Dynamic instability of individual, MAP-free microtubules analyzed by video light microscopy: rate constants and transition frequencies, J. Cell Biol. 107 (1988) 1437–1448.

[6] D. Panda, J.E. Daijo, M.A. Jordan, L. Wilson, Kinetic stabilization of microtubule dynamics steady state in vitro by substoichiometric concentrations of tubulin-colchicine complex, Biochemistry 34 (1995) 9921–9929.
[7] M.A. Jordan, L. Wilson, Microtubules and actin filaments: dynamic targets for cancer chemotherapy, Curr. Opin. Cell Biol. 10 (1998) 123–130.
[8] M. Dogterom, S. Leibler, Physical aspects of the growth and regulation of microtubule structures, Phys. Rev. Lett. 70 (1993) 1347–1350.
[9] F. Gittes, B. Mickey, J. Nettleton, J. Howard, Flexural rigidity of microtubules and actin filaments measured from thermal fluctuations in shape, J. Cell Biol. 120 (1993) 923–934.
[10] B. Mickey, J. Howard, Rigidity of microtubules is increased by stabilizing agents, J. Cell Biol. 130 (1995) 909–917.
[11] E. Krauhs, M. Little, T. Kempf, R. Hofer-Warbinek, W. Ade, H. Ponstingl, Complete amino acid sequence of beta-tubulin from porcine brain, Proc. Natl. Acad. Sci. 78 (1981) 4156–4160.
[12] S. Lobert, L. Hiser, J. Correia, Expression profiling of tubulin isotypes and microtubule-interacting proteins using real-time polymerase chain reaction, Methods Cell Biol. 95 (2010) 47–58.
[13] E.C. Raff, J.D. Fackenthal, J.A. Hutchens, H.D. Hoyle, et al., Microtubule architecture specified by a β-tubulin isoform, Science 275 (1997) 70–73.
[14] O. Behnke, A. Forer, Evidence for four classes of microtubules in individual cells, J. Cell Sci. 2 (1967) 169–192.
[15] N.I. Bughio, G.M. Faubert, R.K. Prichard, Identification of tubulin isoforms in different tissues of *Ascaris suum* using anti-tubulin monoclonal antibodies, Int. J. Parasitol. 21 (1991) 913–918.
[16] P.J. Hussey, N. Haas, J. Hunsperger, et al., The beta-tubulin gene family in Zea mays: two differentially expressed beta-tubulin genes, Plant Mol. Biol. 15 (1990) 957–972.
[17] D. Wang, A. Villasante, S.A. Lewis, N.J. Cowan, The mammalian β-tubulin repertoire: hematopoietic expression of a novel, heterologous β-tubulin isotype, J. Cell Biol. 103 (1986) 1903–1910.
[18] R.F. Luduena, Are tubulin isotypes functionally significant, Mol. Biol. Cell 4 (1993) 445–457.
[19] A. Banerjee, M.C. Roach, P. Tracka, R.F. Luduena, Increased microtubule assembly in bovine brain tubulin lacking the type III isotype of beta-tubulin, J. Biol. Chem. 265 (1990) 1794–1799.
[20] R.D. Burgoyne, M.A. Cambray-Deakin, S.A. Lewis, et al., Differential distribution of beta-tubulin isotypes in cerebellum, EMBO J. 7 (1988) 2311–2319.
[21] K. Shalli, I. Brown, S.D. Heys, et al., Alterations of β-tubulin isotypes in breast cancer cells resistant to docetaxel, FASEB J. 19 (2005) 1299–1301.
[22] C. Tseng, J.Y. Mane, P. Winter, et al., Quantitative analysis of the effect of tubulin isotype expression on sensitivity of cancer cell lines to a set novel colchicine derivatives, Mol. Cancer 9 (2010) 131.
[23] C.N. Newton, J.G. DeLuca, R.H. Himes, et al., Intrinsically slow dynamic instability of Hela cell microtubules *in Vitro*, J. Biol. Chem. 277 (2002) 42456–42462.
[24] J.T. Huzil, K. Chen, L. Kurgan, et al., The roles of β-tubulin mutations and isotype expression in acquired drug resistance, Cancer Inf. 3 (2007) 159–181.
[25] A. Banerjee, Increased levels of tyrosinated alpha-, beta (III)-, and beta (IV)-tubulin isotypes in paclitaxel-resistant MCF-7 breast cancer cells, Biochem. Biophys. Res. Commun. 293 (2002) 598–6019.
[26] R.C. Moore, M. Zhang, L. Cassimeris, R.J. Cyr, In vitro assembled plant microtubules exhibit a high state of dynamic instability, Cell Motil. Cytoskelet. 38 (1997) 278–286.
[27] M.S. Feizabadi, K. Mutafopulos, A. Behr, Measuring the persistence length of MCF7 cell microtubules *in vitro*, Biotechnol. J. 6 (2011) 882–887.
[28] C. Dumontet, M.A. Jordan, F.Y. Lee, Ixabepilone: targeting βIII-tubulin expression in taxane-resistant malignancies, Mol. Cancer Ther. 8 (2009) 17–25.
[29] N. Hirokawa, Y. Noda, Y. Tanaka, S. Niwa, Kinesin superfamily motor proteins and intracellular transport, Nat. Rev. Mol. Cell Biol. 10 (2009) 682–696.
[30] D.A. Skoufias, J.M. Scholey, Cytoplasmic microtubule-base motor proteins, Curr. Opin. Cell Biol. 5 (1993) 95–107.
[31] R.D. Vale, Microtubule motors: many new models off the assembly line, Trends Biochem. Sci. 17 (1992) 300–304.
[32] R. Mallik, S.P. Gross, Molecular motors: strategies to get along, Curr. Biol. 14 (2004) 971–982.
[33] A.W. Hunter, L. Wordeman, How motor proteins influence microtubule polymerization dynamics, J. Cell Sci. 113 (2000) 4379–4389.
[34] M. Sirajuddin, L.M. Rice, R.D. Vale, Regulation of microtubule motors by tubulin isotypes and post-translational modifications, Nat. Cell Biol. 16 (2014) 335–344.
[35] R. Mallik, B.C. Carter, S.A. Lex, et al., Cytoplasmic dynein functions as a gear in response to load, Nature 427 (2004) 649–652.
[36] R. Mallik, D. Petrov, S.A. Lex, et al., Building complexity: an in vitro study of cytoplasmic dynein with in vivo implications, Curr. Biol. 15 (2005) 2075–2085.
[37] M. Vershinin, B.C. Carter, D.S. Razafsky, et al., Multiple-motor based transport and its regulation by Tau, Proc. Natl. Acad. Sci. U.S.A. 104 (2007) 87–92.
[38] Y. Jun, S.K. Tripathy, B.R.J. Narayanareddy, et al., Calibration of optical tweezers for in vivo force measurements: how do different approaches compare?, Biophys J. 107 (2014) 1474–1484.
[39] K.S. Thorn, J.A. Ubersax, R.D. Vale, Engineering the processive run length of the kinesin motor, J. Cell Biol. 151 (2000) 1093–1100.
[40] J. Xu, Z. Shu, S.J. King, S.P. Gross, Tuning multiple motor travel via single motor velocity, Traffic 13 (2012) 1198–1205.
[41] B. Milic, J.O.L. Andreasson, W.O. Hancock, S.M. Block, Kinesin processivity is gated by phosphate release, PNAS 111 (2014) 14136–14140.
[42] L. Hiser, A. Aggarwal, R. Young, et al., Comparison of β-tubulin mRNA and protein levels in 12 human cancer cell lines, Cell Motil. Cytoskelet. 63 (2006) 41–52.
[43] A. Banerjee, R.F. Luduena, Kinetics of colchicine binding to purified beta-tubulin isotypes from bovine brain, J. Biol. Chem. 267 (1992) 13335–13339.
[44] Z. Wang, M.P. Sheetz, The C-terminus of tubulin increases cytoplasmic dynein and kinesin processivity, Biophys. J. 78 (2000) 1955–1964.
[45] T. Luchko, J.T. Huzil, M. Stepanova, J. Tuszynski, Conformational analysis of the carboxy-terminal tails of human beta-tubulin isotypes, Biophys. J. 94 (2008) 1971–1982.
[46] C. Prodromou, B. Panaretou, S. Chohan, et al., The ATPase cycle of Hsp90 drives a molecuar 'clamp' via transient dimerization of N-terminal domains, EMBO J. 19 (2000) 4383–4393.
[47] J. Atherton, I. Farabella, I. Yu, S.S. Rosenfeld, Conserved mechanisms of microtubule-stimulated ADP release, ATP binding, and force generation in transport kinesins, eLife 3 (2014) e03680.